PHYSICAL REVIEW C VOLUME 53, NUMBER 1 JANUARY 1996

The $i_{13/2}$ proton intruder orbital in the superdeformed ^{193}Tl nucleus: Effective magnetic moment and blocking of proton pairing

S. Bouneau,[1] A. N. Wilson,[2] F. Azaiez,[1] J. F. Sharpey-Schafer,[3,4] A. Korichi,[1] I. Deloncle,[5] M. G. Porquet,[5] J. Timar,[6]
A. Astier,[7] M. Bergstrom,[2] C. Bourgeois,[1] L. Ducroux,[7] J. Duprat,[1] B. J. P. Gall,[3] F. Hannachi,[5] M. Kaci,[5] Y. Le Coz,[7]
A. Lopez-Martens,[5] M. Meyer,[7] E. S. Paul,[2] N. Perrin,[1] S. Pilotte,[3] N. Redon,[7] M. A. Riley,[8] C. Schuck,[5] H. Sergolle,[1]
and R. Wyss[9]

[1]*Institut de Physique Nucléaire, Orsay, Institut National de Physique Nucléaire et de Physique des Particules, Centre National de la Recherche Scientifique, F-91406 Orsay Cedex, France*
[2]*Oliver Lodge Laboratory, University of Liverpool, Liverpool, L693BX, United Kingdom*
[3]*Centre de Recherches Nucleaires, Strasbourg, F-67037 Strasbourg Cedex 2, France*
[4]*National Accelerator Centre, P.O. Box 72, Faure, ZA-7B1 South Africa*
[5]*Centre de Spectrometrie Nucléaire et de Spectrometrie de Masse, Institut National de Physique Nucléaire et de Physique des Particles, Centre National de la Recherche Scientifique, F-91405 Orsay Cedex, France*
[6]*Institute of Nuclear Research of the Hungarian Academy of Sciences, H-4001 Debrecen, Hungary*
[7]*Institut de Physique Nucléaire Lyon, Institut National de Physique Nucléaire et de Physique des Particules, Centre National de la Recherche Scientifique, F-69622 Villeurbanne, France*
[8]*Department of Physics, Florida State University, Tallahassee, Florida 32306*
[9]*Physics Department Frescati, The Royal Institute of Technology, Frescativagen 24, S-104 05 Stockholm, Sweden*

(Received 31 July 1995)

From the observed competition between $M1$ and $E2$ γ transitions deexciting the states of the two signature partner yrast superdeformed bands in ^{193}Tl, the $i_{13/2}$ $(\Omega=5/2)$ intruder proton orbital is found to have $(g_K-g_R)K/Q_0=0.138\pm0.008$. A model dependent value of $g_s^{\rm eff}=(0.7\pm0.2)g_s^{\rm free}$ is deduced. A saturation of the $\mathscr{T}^2$ moments of inertia, at rotational frequency $\hbar\omega>0.32$ MeV, is observed for the two bands. This feature is discussed in terms of exhausted quasineutron alignment in the presence of substantially reduced quasiproton alignment due to Pauli blocking.

PACS number(s): 21.10.Re, 21.10.Ky, 21.60.Cs, 27.80.+w

More than 40 rotational bands characteristic of superdeformed (SD) nuclei are now known to exist in Au, Hg, Tl, and Pb isotopes with $A\approx190$ [1]. Recently this mass region of superdeformation has been extended to Bi and Po isotopes [2,3]. A striking difference between the SD nuclei of the 190 mass region and those in other mass regions is the behavior of the dynamic moment of inertia $\mathscr{T}^2$. While the $\mathscr{T}^2$ patterns of the SD bands near $A\approx130$ and 150 show pronounced differences (closely correlated to the high-N proton and neutron intruder orbital occupancy), the majority of the SD bands in the 190 mass region display the same large, smooth increase of $\mathscr{T}^2$ in the rotational frequency range $0.15<\hbar\omega<0.40$ MeV. This behavior of $\mathscr{T}^2$ has been interpreted [4,5] as resulting from the gradual alignment of quasiparticles occupying high-N intruder orbitals (originating from the $i_{13/2}$ proton and $j_{15/2}$ neutron orbitals) in the presence of pair correlations. In this picture, Pauli blocking of high-N intruder orbitals is expected to induce a flattening of the $\mathscr{T}^2$ moments of inertia. Such effects are indeed observed in some odd-Hg [6,7] and odd-Pb [8,9] SD nuclei, where the blocking of the $N=7$ quasineutron or $N=6$ quasiproton alignment is thought to be responsible for the flattening of the $\mathscr{T}^2$ moments of inertia. In some odd-odd Tl isotopes [10,11], the blocking effects of both the $N=7$ quasineutron and $N=6$ quasiproton are also observed. A direct consequence of this interpretation would be that, after the quasiparticle alignments have taken place, the $\mathscr{T}^2$ will exhibit a saturation toward a rigid-body value. Indeed, an onset of saturation of the $\mathscr{T}^2$ has been observed in ^{192}Hg [12], and even more significantly a marked decrease of the $\mathscr{T}^2$ was seen in ^{194}Hg [13], for rotational frequencies $\hbar\omega>0.4$ MeV. In the present work, from the study of their magnetic properties, the two yrast SD bands in ^{193}Tl [14] have been unambiguously assigned to the configuration where the single proton is occupying the $i_{13/2}$ intruder orbital. The two bands have been extended to higher rotational frequencies and their moments of inertia have been found to exhibit a saturation for $\hbar\omega>0.32$ MeV, reflecting the combined effects of the proton pairing blocking and the complete $j_{15/2}$ neutron alignment. Furthermore, a model dependent value of $(g_K-g_R)K/Q_0$ has been obtained with considerable accuracy for the $i_{13/2}$ $(\Omega=5/2)$ proton intruder orbital and the proton effective g_s value in the SD ^{193}Tl has been deduced. This represents the first estimate of the strength of the effective magnetic operator in a rotating very deformed field, which has been a question of discussion for a long time [15–20].

The experiment was carried out at the newly operating Vivitron tandem accelerator at CRN Strasbourg. Excited states in ^{193}Tl were populated with the reaction ^{181}Ta(^{18}O,6n) ^{193}Tl at a beam energy of 110 MeV. The target consisted of a stack of two self-supporting ($\approx$500 μg/cm^2) ^{181}Ta foils. The γ rays emitted in the reaction were detected with the EUROGAM2 detector array [21], consisting of 126 Compton-suppressed Ge detectors (24 quad-clover and 30 large volume Ge detectors). In order to have the full efficiency of the array for low energy γ rays, no absorbers have

0556-2813/96/53(1)/9(5)/$06.00

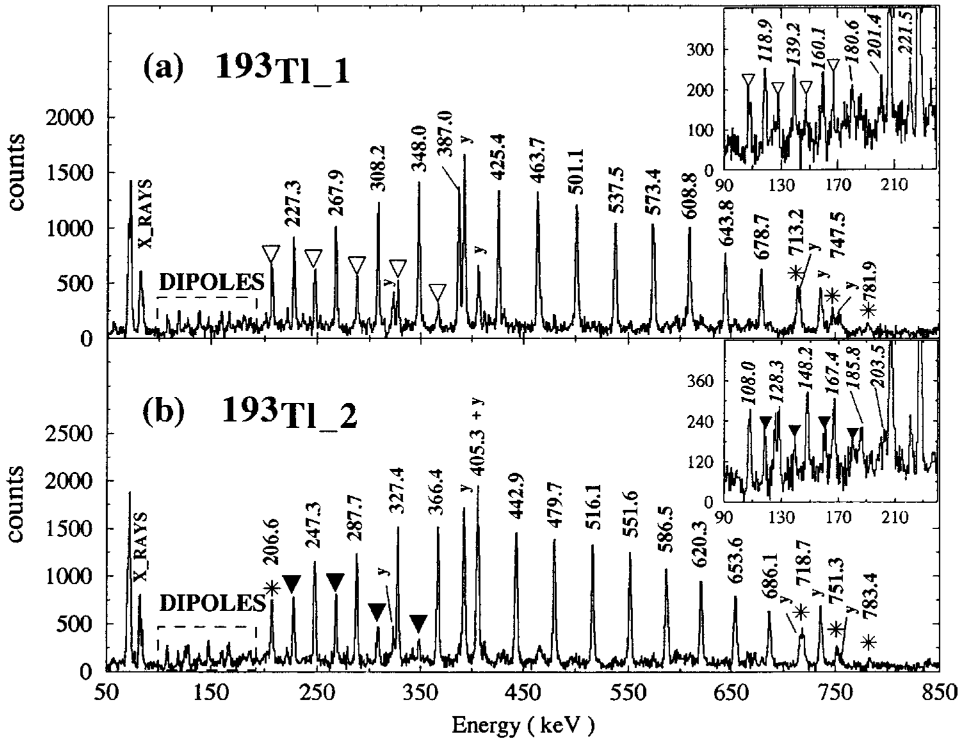

FIG. 1. Spectra of SD bands 1 and 2 in ^{193}Tl. The spectra are from quadrupole coincidences showing γ rays in coincidence with three γ rays that are in the band of interest; (a) band 1 (all indicated transitions of band 1 are used as gates except the 227 and 782 keV); γ transitions in band 2 in coincidence with band 1 are indicated by empty triangles. (b) Band 2 (all indicated transitions of band 2 are used as gates except the 207, 247, 751, and 783 keV); γ transitions in band 1 in coincidence with band 2 are indicated by solid triangles. The dipole transitions linking band 1 and band 2 are indicated in boxes. The γ transitions connecting low-lying normal deformed states are labeled by "*y*." The newly observed transitions are indicated by stars for both bands. Typical uncertainties for $E2$ transition energy are 0.3–0.5 keV.

been used in front of the detectors. Approximately 0.8×10^9 γ-ray coincidence events were recorded to tape for which at least 5 unsuppressed Ge detectors had fired. After unfolding, a total of 8×10^9 quadruple-suppressed γ^4 coincidences were obtained. In addition to the two known yrast SD bands, three excited SD bands have been discovered in the ^{193}Tl nucleus [22]. The triple-gated spectra of the two signature partner yrast SD bands in ^{193}Tl, obtained in the present experiment, are displayed in Fig. 1. All transitions reported earlier [14,23] are clearly observed, together with known ^{193}Tl yrast transitions [24] associated with the decay out of the SD bands. The higher selectivity of the EUROGAM2 array enables us to extend the bands to higher and lower transition energies. In the spectrum of band 1 [Fig. 1(a)], γ transitions of band 2 can clearly be seen up to $\approx$400 keV. The corresponding cross-talk transitions are seen at energies ranging from 100 keV to 200 keV, as indicated in Fig. 1(a). In the spectrum of band 2 [Fig. 1(b)], the situation is reversed and transitions in band 1 are seen, as well as cross-talk transitions. Information on transition multipolarities has been obtained by measuring the ratio of the γ-ray intensities detected in the clover detectors, near 90°, to the intensities detected in the single detectors nearer 0° and 180° to the beam direction. This ratio indicates that the cross-talk transitions are of $\Delta L=1$ type in contrast with the $\Delta L=2$ in-band transitions. The interband transitions together with the transitions in band 1 and band 2 can be organized in a unique way as shown in Fig. 2(a) . Having in mind the fact that band 1 and band 2 are probably signature partners [14,23], it is therefore suggested that in this case, the two-way cross talk would most likely indicate the presence of $M1$ decays. This assumption is corroborated by the evaluation of the conversion coefficient values extracted from total intensity conservation [Fig. 2(b)].

In order to extract the $M1$ strengths from the $I_\gamma(M1)/I_\gamma(E2)$ branching ratios, two different methods have been used. In both methods this has been done in a region of the bands where no signature splitting is present and where one may neglect the contribution of the $K=1/2$ component due to Coriolis mixing. The details of the first method are described in Ref. [25]. In this method we assume there is no decay out from the SD states to the normal deformed states and, provided a proper gating procedure is used, one can obtain an expression for $(g_K-g_R)^2K^2/Q_0^2$ which, in addition to the theoretical total internal conversion coefficients (taken from Ref. [26]), involves only the intensities of the $E2$ γ transitions in both signature partner bands. This procedure has been applied and values of the ratio $(g_K-g_R)^2K^2/Q_0^2$ have been extracted for several SD states in both bands. Figure 3(a) shows the deduced $(g_K-g_R)K/Q_0$ values for different levels of the two signature partner bands as a function of their evaluated spins. The spins of the SD states are suggested using the methods of Draper *et al.* [27] and Becker *et al.* [28]. The details of the second method are described in Ref. [29], where the $(g_K-g_R)K/Q_0$ values are directly extracted from the measured $I_\gamma(M1)/I_\gamma(E2)$ ratios. Figure 3(b) shows the measured $I_\gamma(M1)/I_\gamma(E2)$ for the two SD bands in ^{193}Tl as a function of A, where A represents the dependence on energy and Clebsch-Gordan coefficients of the $M1/E2$ branching ratio $(A=[E_\gamma(M1)^3\times\langle IK10|I-1K\rangle^2]/[E\gamma(E2)^5\times\langle IK20|I-2K\rangle^2])$. Taking the quadrupole moment $Q_0=19\pm2$ eb, which is the average of the measured quadrupole moments in the neighboring ^{192}Hg [30–32] and ^{194}Pb [33] nuclei, we have indicated in Figs. 3(a) and 3(b) by dashed and long-dashed lines the theoretical limits [34] for the configurations where the single proton is occupying the orbitals [642]5/2 and [514]9/2, respectively (the limits come from the uncertainty on the adopted experimental Q_0 value). These are presumably the two lowest strongly coupled orbitals available for the single proton in the thallium isotopes [35–37]. The results from both meth-

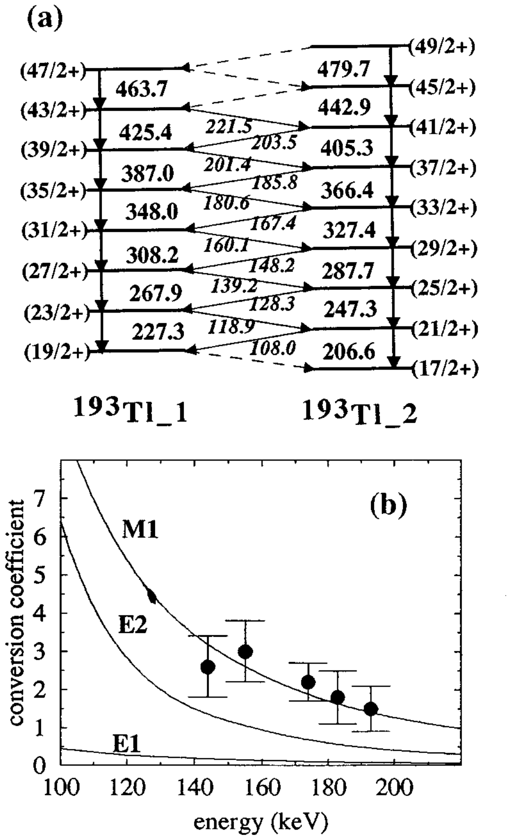

FIG. 2. (a) Low energy part of the level scheme for the pair of signature partner bands in ^{193}Tl. The energies of the dipole transitions (shown in boxes in Fig. 1) are assigned within a 0.2–0.3 keV uncertainty. Dotted arrows indicated unobserved cross-talk dipole transitions. (b) The total internal conversion coefficients for the interband dipole transitions linking the two signature partner SD bands in ^{193}Tl have been deduced from the total intensity conservation. The solid curves represent the theoretical total internal conversion coefficients dependence on transition energy for $M1$, $E1$, and $E2$ transitions [25].

ods are in agreement with the assignment of the intruder configuration [642]5/2 (with both signatures) to the two SD yrast bands in ^{193}Tl. The agreement between the two methods, where one of them is based on the use of theoretical $M1$ internal conversion coefficients for the interband transitions, could be taken as evidence of the magnetic character of those dipole transitions, which is nicely illustrated in Fig. 2(b). The average $(g_K-g_R)K/Q_0$ value obtained from the two methods was found to be equal to 0.138±0.008. Subsequently, the corresponding experimental g_K value would be 1.46±0.17 if the g_R factor is taken equal to Z/A (this value of g_R is quite conventional for normal deformations and justified in part by cranking estimates made by Semmes *et al.* [34]). It is worth pointing out that, despite the very good accuracy of the branching ratio measurements (6%), the accuracy of the extracted values for g_K is always limited by the accuracy of Q_0. In the strong coupling limit of the particle-plus-rotor model, the g_K factor can be expressed as $g_l+[(g_s-g_l)/\Omega]\times\langle s_Z\rangle$ where $\langle s_Z\rangle$ is the expectation value of the intrinsic spin projection on the symmetry axis. The theoretical values of $\langle s_Z\rangle$ for a pure $i_{13/2}$ ($\Omega=5/2$) proton configuration obtained with Hartree-Fock [36] and Woods-Saxon calculations

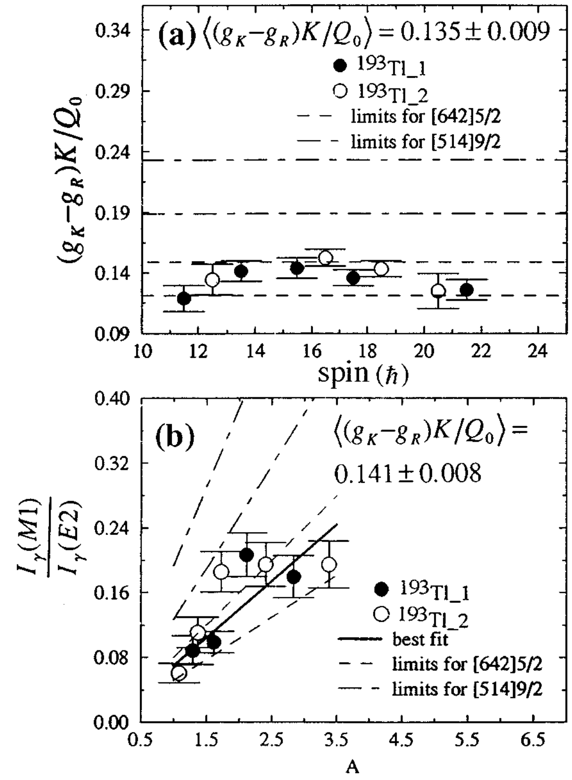

FIG. 3. (a) The $(g_K-g_R)K/Q_0$ values (extracted indirectly, see text) for SD states in band 1 and band 2 of ^{193}Tl (the units are μ_N/eb) as a function of their evaluated spins. (b) Measurements of the $I_\gamma(M1)/I_\gamma(E2)$ branching ratio taken on band 1 and band 2, plotted as a function of A $(A=[E_\gamma(M1)^3\times\langle IK10|I-1K\rangle^2]/[E_\gamma(E2)^5\langle IK20|I-2K\rangle^2])$. Taking $Q_0=19\pm2$ eb, the theoretical [33] limits are indicated for [514]9/2$^-$, $g_K=1.31$ (long dashed lines) and the [642]5/2$^+$, $g_K=1.45$ (dashed lines) proton configurations. The theoretical limits come from the uncertainty on the experimental quadrupole moment.

[34] are found to be in excellent agreement. These values are $\langle s_Z\rangle=0.4$ and $\langle s_Z\rangle=0.39$, respectively. Using $\langle s_Z\rangle=0.4$, the renormalization factor for the magnetic moment due to the intrinsic spin $g_s^{\text{eff}}/g_s^{\text{free}}$ was found to be equal to 0.7±0.2 (considering only the uncertainties on the experimental values of g_K and Q_0). It is worth pointing out that the observed values of g_K for normal deformed odd-A nuclei $(150<A<190)$ indicate a polarization effect of the same magnitude of $g_s^{\text{eff}}\approx0.7g_s^{\text{free}}$ [38]. This represents the first experimental estimate of the effective magnetic operator in a superdeformed nucleus at high spin.

With the extension of the two SD bands toward higher energies, it is now possible to extend the dynamic moments of inertia $\mathcal{J}^2$ up to frequencies $\hbar\omega\approx0.4$ MeV as is shown in Fig. 4. For both bands a change in slope of the $\mathcal{J}^2$ with $\hbar\omega$ is noticeable at low ($\hbar\omega\approx0.15$ MeV) and high ($\hbar\omega\approx0.32$ MeV) frequencies. Furthermore, a smooth turnover of the $\mathcal{J}^2$'s can be seen around $\hbar\omega\approx0.36$ MeV. The $\mathcal{J}^2$ moments of inertia of the vacuum SD bands in the neighboring even-even isotones ^{192}Hg [12] and ^{194}Pb [39] are displayed for comparison in the same figure. At low frequencies these zero-quasiparticle SD bands have reduced $\mathcal{J}^2$ values compared with the one-quasiparticle bands in ^{193}Tl. This is what one expects for odd nuclei: a substantial increase of the moment

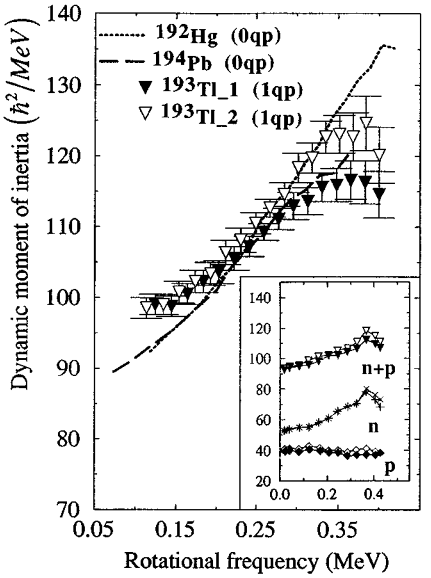

FIG. 4. Experimental dynamic moments of inertia as a function of $\hbar\omega$ for the SD bands: ^{193}Tl 1 (solid triangle), ^{193}Tl 2 (empty triangle), ^{192}Hg (dotted line), ^{194}Pb (dashed line). The inset shows results from new theoretical calculations [39] for the yrast SD configuration ($\pi i_{13/2}$) in ^{193}Tl. The three sets of curves in the inset represent the calculated total $\mathscr{J}^2$ values and their decomposition into neutron and proton contributions for both signature partners of the [642]5/2$^+$ orbital.

of inertia due to the well-known blocking effect that reduces superfluidity and hence increases $\mathscr{J}^2$. At intermediate rotational frequencies 0.2 MeV$<\hbar\omega<$0.3 MeV, all the SD bands shown in Fig. 4 exhibit roughly the same increase of $\mathscr{J}^2$. Generally this increase is qualitatively understood in the 190 mass region in terms of gradual alignment of $\nu j_{15/2}$ and $\pi i_{13/2}$ in the presence of pairing correlations [4,5]. Having in mind that the $i_{13/2}$ proton orbital is blocked for pairing correlations in the ^{193}Tl SD bands, the relatively small differences in the $\mathscr{J}^2$ between^{192}Hg, ^{193}Tl, and ^{194}Pb (see Fig. 4) can be taken as evidence for a relatively small contribution of the $\pi i_{13/2}$ quasiparticle alignment to the increase of the moment of inertia. In other words, it is mainly the $\nu j_{15/2}$ quasiparticle which contributes to the rise of $\mathscr{J}^2$ at the intermediate rotational frequency range (0.2 MeV$<\hbar\omega<$0.3 MeV). This is confirmed by recent studies of the SD odd-Pb isotopes, where the blocking of the $j_{15/2}$ neutron orbital was found to affect the flattening of the $\mathscr{J}^2$ moments of inertia [8,9] more dramatically than in the SD odd-Hg isotopes [6,7]. Furthermore, the $\mathscr{J}^2$ moment of inertia of the vacuum SD band in ^{194}Pb exhibits the same slope at intermediate rotational frequencies as band 1 in ^{193}Tl. This suggests that pairing correlations for protons are weaker in Pb isotopes than in Hg isotopes. The saturation of the $\mathscr{J}^2$ at $\hbar\omega\approx$0.32 MeV in ^{193}Tl SD bands indicates that the alignment of the $j_{15/2}$ neutron quasiparticle is exhausted. In the ^{192}Hg vacuum SD band the $i_{13/2}$ quasiparticle alignment takes over and the $\mathscr{J}^2$ continues to increase until a beginning of saturation at $\hbar\omega\approx$0.4 MeV. It is worth pointing out that recent theoretical calculations, where deformation and pairing effects are treated self-consistently by means of the cranked Strutinsky Lipkin-Nogami approach and where a quadrupole pairing interaction is included [40], reproduce very well the dynamic moment of inertia of the yrast SD bands in ^{193}Tl (see the inset of Fig. 4).

To summarize, we have observed dipole transitions between signature partner bands in the SD ^{193}Tl nucleus. This enables us to measure $M1$ strengths and to extract the g_K factor for the $\pi i_{13/2}$ ($\Omega=5/2$) orbital. A model dependent strength of the effective magnetic operator in a rotating superdeformed nucleus is deduced for the first time. From the comparison to the SD ^{192}Hg core, the Pauli blocking effect generated by the occupancy of the $\pi i_{13/2}$ orbital is found to produce a fairly different behavior of the $\mathscr{J}^2$ moments of inertia as a function of rotational frequency. In particular, a saturation of the $\mathscr{J}^2$ moments of inertia at relatively low rotational frequency $\hbar\omega\approx$0.32 MeV is observed for the two yrast SD bands in ^{193}Tl, illustrating a completed $j_{15/2}$ quasineutron alignment and/or a substantial reduction of neutron pairing correlations at large rotational frequencies ($\hbar\omega$ $>$0.32 MeV).

We are thankful to all those responsible from CRN Strasbourg for the operation of the Vivitron. We also would like to thank all those involved in the setting up and commissioning of EUROGAM2, especially D. Curien, G. Duchene, and G. de France. The EUROGAM project was funded jointly by EPSRC (UK) and IN2P3 (France).

---

[1] R. B. F. Firestone and B. Singh, "Table of Superdeformed Nuclear Bands" (unpublished).
[2] R. M. Clark *et al.*, Phys. Rev. C **51**, R1052 (1995).
[3] D. McNabb *et al.* (unpublished).
[4] M. A. Riley *et al.*, Nucl. Phys. **A512**, 178 (1990).
[5] M. W. Drigert *et al.*, Nucl. Phys. **A530**, 452 (1992).
[6] M. J. Joyce, Phys. Lett. B **340**, 150 (1994).
[7] M. P Carpenter *et al.*, Phys. Rev. C **51**, 2400 (1995).
[8] J. R. Hughes *et al.*, Phys. Rev. C **51**, R447 (1995).
[9] L. P. Farris *et al.*, Phys. Rev. C **51**, R2288 (1995).
[10] Y Liang *et al.*, Phys. Rev. C **46**, R2136 (1992).
[11] F. Azaiez *et al.*, Phys. Rev. Lett. **66**, 1030 (1991); J. Duprat *et al.* (unpublished).
[12] B. J. P. Gall *et al.*, Z. Phys. A **347**, 223 (1994).
[13] B. Cederwall *et al.*, Phys. Rev. Lett. **72**, 3150 (1994).
[14] F. B. Fernandez *et al.*, Nucl. Phys. **A517**, 386 (1990).
[15] I. Hamamoto and W. Ogle, Nucl. Phys. **A240**, 54 (1975).
[16] V. Metag, D. Habs, and H. J. Specht, Phys. Rep. **65**, 1 (1980).
[17] J. Libert, M. Meyer, and P. Quentin, Phys. Lett. **95B**, 175 (1980).
[18] J. Libert, M. Meyer, and P. Quentin, Phys. Rev. C **25**, 586 (1982).
[19] I. Hamamoto and W. Nazarewicz, Phys. Lett. B **297**, 25 (1992).
[20] U. Hofmann and P. Ring, Phys. Lett. B **214**, 307 (1988).

[21] P. J. Nolan, F. A. Beck, and D. B. Fossan, Annu. Rev. Nucl. Part. Sci. **44**, 561 (1994).

[22] J. F. Sharpey-Schafer *et al.*, contribution to the XXXIII Winter Meeting on Nuclear Physics, Bormio, Italy, January 1995.

[23] J. Duprat *et al.*, in *International Conference on the Future of Nuclear Spectroscopy, Crete, Greece*, edited by W. Gelletly, C. A. Kalfas, R. Vlastou, S. Harissopulos, and D. Loukas (1993), p. 199.

[24] W. Reviol *et al.*, Nucl. Phys. **A452**, 351 (1992).

[25] J. Duprat *et al.*, Phys. Lett. B **341**, 6 (1994).

[26] F. Rosel *et al.*, At. Data Nucl. Data Tables **21**, 91 (1978).

[27] J. E. Draper *et al.*, Phys. Rev. C **42**, R1791 (1990).

[28] J. A. Becker *et al.*, Phys. Rev. C **46**, 889 (1992).

[29] M. J. Joyce *et al.*, Phys. Rev. Lett. **71**, 2176 (1993).

[30] E. F. Moore *et al.*, Phys. Rev. Lett. **65**, 3127 (1990).

[31] P. Willsau *et al.*, Nucl. Phys. **A574**, 56 (1994).

[32] A. Korichi *et al.*, Phys. Lett. B **345**, 403 (1995).

[33] P. Willsau *et al.*, Z. Phys. A **344**, 351 (1993).

[34] P. B. Semmes *et al.*, Phys. Lett. B **345**, 185 (1995); and (private communication).

[35] W. Satula *et al.*, Nucl. Phys. **A 529**, 289 (1990).

[36] M. Meyer *et al.*, Phys. Rev. C **45**, 233 (1992); and (private communication).

[37] B. Gall*et al.*, Z. Phys. A **348**, 183 (1994).

[38] A. Bohr and B. R. Mottelson, *Nuclear Structure* (Addison-Wesley, Reading, MA, 1975), Vol. 2, p. 303.

[39] B. J. P. Gall *et al.*, Phys. Lett. B **345**, 124 (1995).

[40] W. Satula and R. Wyss, Phys. Rev. C **50**, 2888 (1994), and (private communication).